

# Low Temperature Synthesis of the $x\text{BiScO}_3-(1-x)\text{BaTiO}_3$ , $x=0\div 0.03$ Ferroelectric System

Tatyana Karpova<sup>1,\*</sup>, Victor Vassil'ev<sup>1,2</sup>, Elena Vladimirova<sup>1,2</sup>, Vladimir Shur<sup>3</sup>, Vera Shikhova<sup>3</sup>,  
Vladimir Osotov<sup>4</sup>, Alexander Nosov<sup>4</sup>

<sup>1</sup>Ural Division of RAS, Institute of Solid State Chemistry, Ekaterinburg, 620041, Russia

<sup>2</sup>Ural Federal University named after the first President of Russia B.N. Yeltsin, Institute of  
Material Studies and Metallurgy, Ekaterinburg, 620002, Russia

<sup>3</sup>Ural Federal University named after the first President of Russia B.N. Yeltsin,  
Ferroelectric Laboratory, Ekaterinburg, 620051, Russia

<sup>4</sup>Ural Division of RAS, Institute of Metal Physics, Ekaterinburg, 620041, Russia

---

**Abstract** The ferroelectric ceramic of the  $x\text{BiScO}_3-(1-x)\text{BaTiO}_3$ ,  $x=0\div 0.03$  system was prepared by solid state reaction synthesis at temperatures below 850°C. Solid solutions with tetragonal symmetry were formed. Doping with  $\text{BiScO}_3$  resulted in linear increase with  $x$  the unit cell parameters, maximum temperature of the dielectric constant and its maximum value. Room temperature measurements of ferroelectric properties revealed more complicated behavior on doping with optimum combination of ferroelectric properties for composition with  $x = 0.015$ .

**Keywords** Oxides, Chemical Synthesis, Electron Microscopy, Dielectric Properties

---

## 1. Introduction

The relaxor ferroelectrics with the perovskite  $\text{ABO}_3$  structure are characterized by smeared maximum at the temperature dependence of dielectric constant  $\epsilon$  and its frequency dispersion in the region of phase transition[1]. Optimization of physical properties of these materials can be made by simple or complicated doping of the A or B positions of the perovskite structure[2-4]. The  $\text{BaTiO}_3$ -based ferroelectrics systems attract permanent interest as Pb-free ecologically clean materials[5,6].

An isovalent doping of B sites of the perovskite structure is usually used for tailoring the Curie temperature  $T_C$  and lowering the temperatures of the tetragonal-orthorhombic and orthorhombic-rhombohedral phase transitions. For example, doping by  $\text{Zr}^{4+}$  and  $\text{Sn}^{4+}$  ions results in linear decrease of  $T_C$  and increase of the temperatures of phase transitions[7-9]. Isovalent doping by ions of similar radius does not influence the charge states and no electrical fields appear. Isovalent doping of B-sites by ions with large (~20-30%) difference of ion radius results in appearance of random elastic fields and relaxor properties[9]. Heterovalent doping of B-sites substantially hinders the ordering processes in the perovskite structure and superstructures may appear.

Heterovalent doping of A-sites in the  $\text{BaTiO}_3$  structure may result in both deterioration of ferroelectric order and appearance of relaxor behavior[10], and substantial variation of the temperatures of ferroelectric phase transitions. Substitution of  $\text{Ba}^{2+}$  by  $\text{Bi}^{3+}$  practically does not influence  $T_C$  till doping level of 10%, however abnormal behavior of dielectric constant is observed at bismuth ion concentration of 2%. Such behavior is characteristic of the ferroelectric phase and characterized by substantial frequency dispersion [10].

Simultaneous doping of both A- and B-sites in the  $\text{BaTiO}_3$  structure can be characterized by complicated mechanism of charge compensation and also results in substantial variation of ferroelectric properties: shift of the phase transition temperatures, relaxor behavior at small and low concentrations of doping ions, abnormal behavior of dielectric constant and other physical characteristics. Recent investigations of the  $x\text{BiScO}_3-(1-x)\text{BaTiO}_3$  solid solutions[11,12] showed that they are characterized by high values of the piezoelectric constants and electromechanical coupling factor due to peculiarities of their phase diagram and existence of morphotropic phase boundary. The relaxor behavior is determined by disordering of heterovalent ions in the structurally equivalent sites of crystal lattice.

At room temperature the  $\text{BiScO}_3$  compound has the monoclinic type of lattice symmetry and the question about existence of structural phase transitions still remains open[13]. At present  $\text{BiScO}_3$  is actively used as doping compound in various ferroelectric systems:  $\text{BiScO}_3\text{-PbTiO}_3$  [14],  $(\text{K}_{0.5}\text{Bi}_{0.5})\text{TiO}_3\text{-BiScO}_3\text{-PbTiO}_3$ [15],  $\text{BiScO}_3\text{-(K}_{0.475}$

---

\* Corresponding author:

Geoma2006@yandex.ru (Tatyana Karpova)

Published online at <http://journal.sapub.org/materials>

Copyright © 2011 Scientific & Academic Publishing. All Rights Reserved

$\text{Na}_{0.475}\text{Li}_{0.05})(\text{Nb}_{0.95}\text{Sb}_{0.05})\text{O}_3$ [16].

According to [7,8] the  $x\text{BiScO}_3-(1-x)\text{BaTiO}_3$  solid solutions with perovskite structure are formed for the concentration region  $0 \leq x \leq 0.4$ . For  $0 \leq x \leq 0.05$  such solid solutions have tetragonal structure (the  $P4mm$  space group) with the degree of tetragonality linearly decreasing from 1.0103 (undoped  $\text{BaTiO}_3$ ) to 1.103 ( $x=0.5$ ), such behavior is explained by cumulative effect from simultaneous  $c$  lattice parameter decrease and  $a$  lattice parameter increase. Note that in [8] calculations were made under assumption of equivalent of substitution of Ba and Ti by Bi and Sc ions, respectively, with equal values of the thermal disorder parameters. Coexistence of two phases – tetragonal (space group  $P4mm$ ) and trigonal (space group  $R3m$ ) – is observed for  $0.05 \leq x \leq 0.20$ . The existence of phase with perovskite-like structure (space group  $Pm3m$ ) was observed for  $x > 0.2$ . It was shown that addition of  $\text{BiScO}_3$  may influence the ferroelectric properties of the  $x\text{BiScO}_3-(1-x)\text{BaTiO}_3$  solid solutions [10]: for  $0.02 \leq x \leq 0.10$  substantial variations of the ferroelectric loop shape and remnant polarization were observed. However no data were obtained for lower doping concentrations.

The principal problem of synthesis of Bi-containing oxide compounds using  $\text{Bi}_2\text{O}_3$  as one of the starting components is its relatively low melting temperature  $825^\circ\text{C}$ [17]. Depending on the preparation method the influence of Bi volatility is minimized in different ways. When the samples are prepared by the solid state reactions method, long milling with subsequent anneal at relatively low temperature of  $900^\circ\text{C}$  for the short period of time (2 h.) [18] is used. When the complex oxide compounds are prepared using molten salt synthesis with calcinations in sealed alumina crucibles at  $1100^\circ\text{C}$  for 2 h with subsequent thorough washing with hot deionized water [19]. When the sol-gel method is used for synthesis, the samples are sintered at various temperatures from  $1100$  to  $1150^\circ\text{C}$ , for 1 h in air [20]. When the solid state reactions method is used at higher temperatures ( $1050$ - $1320^\circ\text{C}$ ) and for longer durations (till 20 hours) the samples are prepared in a closed crucible with excess of  $\text{Bi}_2\text{O}_3$  since more than two-thirds of its excess quantity can be evaporated during sintering [10]. The disadvantage of addition of excess quantities of  $\text{Bi}_2\text{O}_3$  during sintering is in possible Bi incorporation into  $\text{BaTiO}_3$ . Such Bi doping of  $\text{BaTiO}_3$  induces a decrease in  $T_c$  as was shown in [21].

In this work the  $x\text{BiScO}_3-(1-x)\text{BaTiO}_3$  solid solutions with  $0.00 \leq x \leq 0.03$  were prepared by solid state reactions method by heat treatment of stoichiometric mixtures of  $\text{BaTiO}_3$ ,  $\text{Bi}_2\text{O}_3$ , and  $\text{Sc}_2\text{O}_3$  in the temperature interval from  $500$  till  $850^\circ\text{C}$ . The structural, dielectric, and ferroelectric properties of thus obtained bulk ceramics were studied.

## 2. Experimental

Powder samples of  $x\text{BiScO}_3-(1-x)\text{BaTiO}_3$ , where  $x = 0, 0.010, 0.015, 0.020, 0.025, 0.030$ , were prepared by conventional solid state reactions method from reagent grade

$\text{BaCO}_3$ ,  $\text{TiO}_2$ ,  $\text{Bi}_2\text{O}_3$ , and  $\text{Sc}_2\text{O}_3$ , taken in stoichiometric proportions. The undoped  $\text{BaTiO}_3$  was synthesized by gradual increase of the sintering temperature from  $800^\circ\text{C}$  to  $1100^\circ\text{C}$  with intermediate grindings. The  $x\text{BiScO}_3-(1-x)\text{BaTiO}_3$  samples were obtained by addition to  $\text{BaTiO}_3$  the stoichiometric amounts of  $\text{Bi}_2\text{O}_3$  and  $\text{Sc}_2\text{O}_3$  mixtures. These mixtures were first mixed in ethanol with the approximately equal quantities of barium titanate, then gradually the rest amount of barium titanate was added till the homogeneous mixture of the desired stoichiometry have been obtained. The mixtures were annealed with increase of the sintering temperature from  $600^\circ\text{C}$  to  $850^\circ\text{C}$  with intermediate grindings. Higher annealing temperatures were deliberately avoided due to volatility of  $\text{Bi}_2\text{O}_3$ . Total duration of sintering at the temperature of  $850^\circ\text{C}$  was 46 hours. All anneals were carried out in air.

X-ray diffraction analysis was performed at room temperature for structural analysis and lattice parameters determination using the Shimadzu XRD-7000 diffractometer with monochromatic  $\text{CuK}\alpha$  radiation ( $\lambda=0,15418$  nm) for the  $2\theta$  interval from  $20^\circ$  to  $80^\circ$  and scan speed  $0.9^\circ/\text{min}$ . Phase identification was carried out using the JCPDS-ICDD cards No.00-005-0626, and No.01-075-3569. Structural parameters were calculated using the FullProf Suite (version 2.00) software. In order to validate correctness of utilization of X-ray diffraction analysis for structural characterization of the  $x\text{BiScO}_3-(1-x)\text{BaTiO}_3$  solid solutions with small doping levels (in our case  $x$  was less than 0.030) special calibration measurements have been made on the unannealed mixtures of  $\text{BaTiO}_3$  with the corresponding quantities of  $\text{Bi}_2\text{O}_3$  and  $\text{Sc}_2\text{O}_3$ . The surface topography of the samples was studied using the JEOL JSM-6390LA scanning electron microscope with X-ray dispersive microanalysis. The size distribution of powder particles was measured using the Horiba partica LA-950V2 laser analyzer. For electrical measurements the powders were cold isostatically pressed at 15 MPa and disk-shaped bulk samples with typical dimensions of 10 mm in diameter and 1-3 mm in thickness were annealed at  $850^\circ\text{C}$  for 6 h. in air. The density of bulk samples was determined by weighing in liquid. For electrical measurements on bulk pellet samples the sintered pellets were polished to achieve parallel, smooth surfaces, and electrodes were made by sintering of the Ag-containing paste at the temperature of  $850^\circ\text{C}$  for 10 min in air. Dielectric measurements were performed from  $30$  to  $190^\circ\text{C}$  in custom designed furnace with Actacom AM-3001 LCR meter. Ferroelectric hysteresis loops were measured at room temperature under the action of triangle ac field with frequency 1 Hz and amplitude up to 33 kV/cm. Pulses of the switching electric field were generated by DAC card PCI-6251 with LabVIEW-based software and amplified by high voltage amplifier TREK 20/2°C. The switching current data were recorded by measuring the signal on the serious resistor of 20 k $\Omega$ . The switching charge was obtained by digital integration of the current data.

## 3. Results and Discussion

Figure 1 shows the X-ray diffraction patterns recorded at room temperature. Their analysis permitted to conclude that the solid solutions are formed and all samples have the tetragonal symmetry (the space group  $P4mm$ ), which correspond to the known data[14,15].

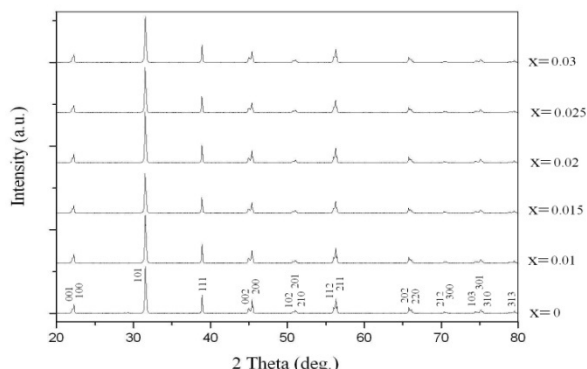


**Figure 1.** X-ray diffraction patterns of the  $x\text{BiScO}_3-(1-x)\text{BaTiO}_3$  samples

The crystal lattice parameters are given in Table 1. In accordance with the Vegard law[16], linear variation of lattice parameters is observed for the  $x\text{BiScO}_3-(1-x)\text{BaTiO}_3$  system with  $x$  increasing from zero to 0.03. The question about sensitivity of X-ray analysis and its applicability for correct determination of structural parameters at small doping levels was clarified by precise measurements on the initial mixtures of  $\text{BaTiO}_3$  with the corresponding quantities of  $\text{Bi}_2\text{O}_3$  and  $\text{Sc}_2\text{O}_3$ . The results obtained for the sample with  $x = 0.01$  just after mixing and after annealing are presented in Fig.2(a) and Fig.2(b) respectively.

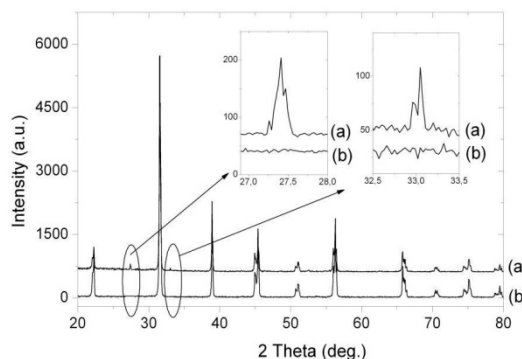
**Table 1.** Crystal Structure Parameters for the  $x\text{BiScO}_3-(1-x)\text{BaTiO}_3$  Samples

$x\text{BiScO}_3-(1-x)\text{BaTiO}_3$	Space group	Symmetry	Lattice constant, (Å)		Volume, Å <sup>3</sup>	Bragg R-factor
			<i>a</i>	<i>c</i>		
$x=0.000$	$P4mm$	Tetragonal	3.99400	4.03116	64.3052	1.43
$x=0.010$			3.99690	4.03480	64.4567	1.68
$x=0.015$			3.99810	4.03580	64.5115	2.80
$x=0.020$			3.99989	4.03720	64.5917	2.85
$x=0.025$			4.00079	4.03800	64.6335	2.72
$x=0.030$			4.00244	4.03871	64.6982	1.52

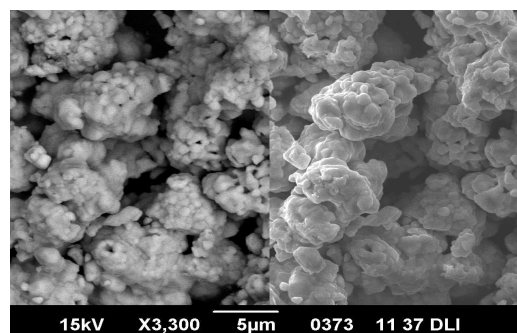
In the diffraction pattern of Fig.2(a) the peaks from  $\text{BaTiO}_3$ ,  $\text{Bi}_2\text{O}_3$ ,  $\text{Sc}_2\text{O}_3$  are clearly seen. In Fig.2(b) the peaks from  $\text{Bi}_2\text{O}_3$  and  $\text{Sc}_2\text{O}_3$  are absent while the peaks corresponding only to the perovskite phase are clearly seen. These data confirm the sufficient sensitivity of our X-ray experimental setup for correct determination of the structural parameters of the  $x\text{BiScO}_3-(1-x)\text{BaTiO}_3$  system with  $x$  below 0.03.

Figure 3 shows the SEM images of the  $0.03\text{BiScO}_3-0.97\text{BaTiO}_3$  sample surface. Analysis of the backscattered image (Fig.3a) permits to conclude that the sample consists of grains with homogeneous phase composition. The secondary electron image (Fig.3b) permits to evaluate the morphology of the samples: after thermal treatment the powders with rounded shapes formed bigger agglomerates. Such

sample surface morphology is typical of the solid state reactions synthesis method.

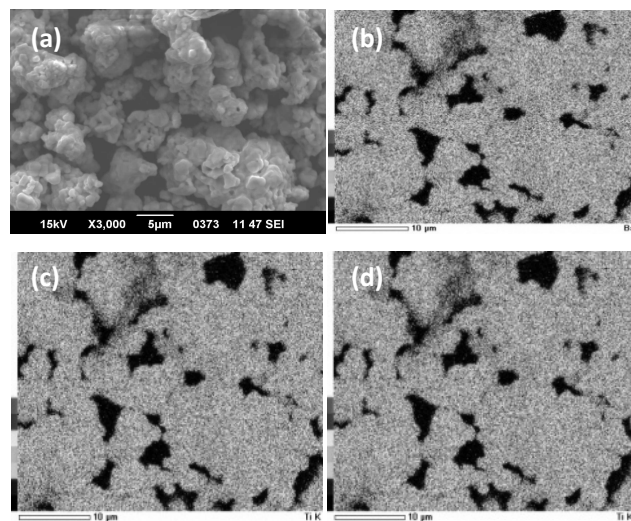


**Figure 2.** X-ray diffraction patterns of the  $x\text{BiScO}_3-(1-x)\text{BaTiO}_3$ ,  $x=0.01$ , just after mixing (a) and after annealing (b) of  $\text{BaTiO}_3$  with the corresponding quantities of  $\text{Bi}_2\text{O}_3$  and  $\text{Sc}_2\text{O}_3$



**Figure 3.** SEM images of the  $0.03\text{BiScO}_3-0.97\text{BaTiO}_3$  sample surface. Backscattered image (a); secondary electron image (b)

Figure 4 shows the results of EDX analysis of the  $0.03\text{BiScO}_3-0.97\text{BaTiO}_3$  sample with distributions of individual elements. Spatial coincidence of these distributions, in particular of Bi, gives additional evidence for phase homogeneity of the samples and substantial reduction of influence of Bi volatility by proper choice of heat treatment temperature. Homogeneous distribution of elements over the sample surface was additionally confirmed by recording and comparing the full EDX spectra in more than 20 points over the image.



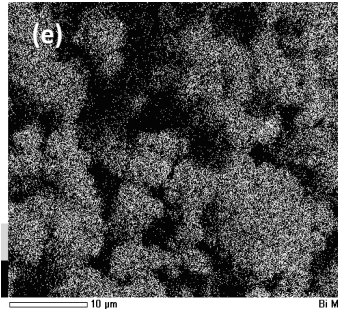


**Figure 4.** SEM-image of the  $0.03\text{BiScO}_3-0.97\text{BaTiO}_3$  sample surface (a) with the results of EDX analysis: spatial distribution of the Ba element (b); spatial distribution of the Ti element (c); spatial distribution of the Sc element (d); spatial distribution of the Bi element (e)

Temperature dependences of dielectric constant  $\varepsilon$  recorded at frequencies of 10 Hz and 100 kHz are shown in Fig. 5. The positions of maxima  $T_{max}$  of  $\varepsilon(T)$  dependences and the maximum values of dielectric constant  $\varepsilon_{max}$  almost linearly increase with the content of  $\text{BiScO}_3$  and corresponding lattice parameters. Such behavior can be attributed to the increasing lattice disorder with  $x$  and probable formation of nanoclusters. Almost no frequency dispersion is observed. The values of  $\varepsilon_{max}$  are lower than those observed, for example, in [10]. This fact is the result of combined influence of two factors: lower sintering temperature and average grain size dependence of  $\varepsilon$ . As was shown in [22] lowering the sintering temperature from  $1200^\circ\text{C}$  to  $900^\circ\text{C}$  results in almost 9 times decrease of  $\varepsilon$  in the vicinity of  $T_{max}$ , while very sharp dependence of  $\varepsilon$  on an average grain size  $d_{av}$  is observed [23]. According to [23] the maximum of  $\varepsilon(d_{av})$  dependence corresponds to  $d_{av} \approx 1 \mu\text{m}$  with  $\approx 2.75$  times drop for  $d_{av}$  increasing from 1 to  $3 \mu\text{m}$ .

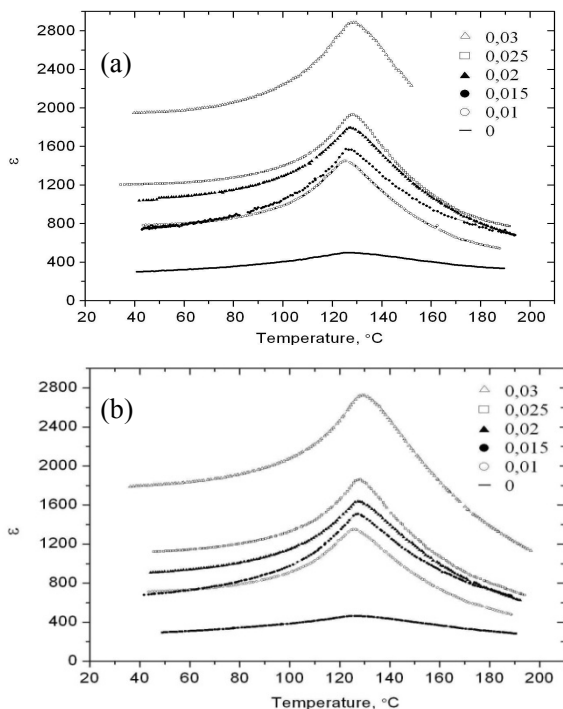


**Figure 5.** Temperature dependences of the dielectric constant for the  $x\text{BiScO}_3-(1-x)\text{BaTiO}_3$  samples recorded at frequencies of 100 Hz (a) and 100 kHz (b)

The inverse of the dielectric constant at 100 kHz as a function of temperature was investigated to confirm whether or not the behavior of  $\varepsilon(T)$  dependences above  $T_{max}$  can be described by the Curie–Weiss law [1]. The 100 kHz data were used to minimize possible space charge contribution to the dielectric constant. It was observed that the Curie–Weiss law is obeyed for all compositions under investigation. The Curie constant  $C_{CW}$  varied linearly with  $x$  from  $C_{CW} = 4.8 \cdot 10^4^\circ\text{C}$  for  $x=0.00$  to  $C_{CW} = 1.4 \cdot 10^5^\circ\text{C}$  for  $x \leq 0.03$ . Such values are comparable with other ferroelectric materials with displacive phase transitions [1]. The observed agreement with the Curie–Weiss law in this system is characteristic of a proper ferroelectric. Since both dielectric dispersion and deviation from the Curie–Weiss law are characteristic of relaxor ferroelectric materials, our results suggest that at small doping levels the  $x\text{BiScO}_3-(1-x)\text{BaTiO}_3$  solid solution behaves like a normal ferroelectric.

Figure 6 shows the ferroelectric loops for the  $x\text{BiScO}_3-(1-x)\text{BaTiO}_3$ ,  $0.00 \leq x \leq 0.03$  system.

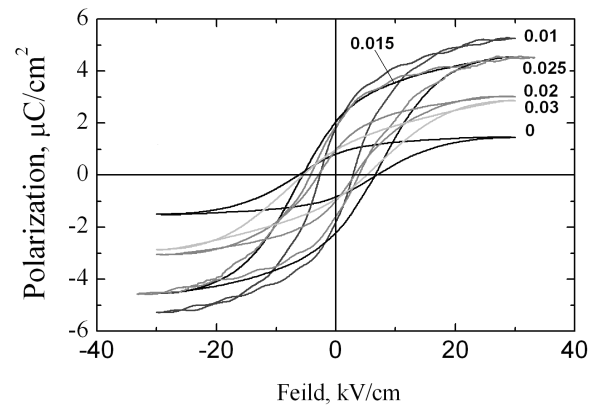


**Figure 6.** Ferroelectric hysteresis loops for the  $x\text{BiScO}_3-(1-x)\text{BaTiO}_3$ ,  $x=0\div 0.03$  samples

The principal characteristics of polarization loops - saturation polarization  $P_s$ , remnant polarization  $P_r$ , and coercive field  $H_c$ , are given in Table 2.

**Table 2.** Physical characteristics of the  $x\text{BiScO}_3-(1-x)\text{BaTiO}_3$  samples.  $\varepsilon_{max}$  - maximum value of the dielectric constant;  $T_{max}$  - temperature of the maximum of the  $\varepsilon(T)$  curve;  $\rho_{rel}$  - relative density (with respect to theoretical X-ray density);  $d_{av}$  - average grain size;  $P_s$  - saturation polarization;  $P_r$  - remnant polarization;  $H_c$  - coercive field

Composition, $x$	$\varepsilon_{max}$		$T_{max}$		$\rho_{rel}$ %	$d_{av}$ $\mu\text{m}$	$P_s$ $\mu\text{C}/\text{cm}^2$	$P_r$ $\mu\text{C}/\text{cm}^2$	$H_c$ $\text{kV}/\text{cm}$
	100 Hz	100 kHz	100 Hz	100 kHz					
0.000	498.41	463.67	124.8	126.1	88.0	1.87	1.32	0.80	6.20
0.010	1449.47	1350.74	124.9	126.6	88.9	1.64	4.87	1.80	2.64
0.015	1569.87	1506.21	125.6	127.4	89.7	1.77	4.10	2.05	5.51
0.020	1793.60	1636.89	126.4	128.3	79.8	1.94	2.81	0.97	2.89
0.025	1929.88	1861.87	126.6	128.9	92.1	1.93	4.09	1.86	4.23
0.030	2886.50	2727.40	128.6	128.8	88.2	1.97	2.48	0.97	5.51

Nonmonotonic dependence on  $x$  is observed. Analysis of these data must be made with an account for the concentration dependence of relative density  $\rho_{rel}$ . For all compositions its values are in the range from 88.0 till 92.1%, except for the sample with  $x=0.020$ . Such small density resulted in

lower values of all parameters of ferroelectric loop. Maximum values of each parameter are observed for different compositions: saturation polarization is maximum for  $x = 0.010$ , remnant polarization is maximum for  $x = 0.015$ , while the coercive field is maximum for the same composition. With an account for the fact that the maximum value of squareness ratio  $Pr/Ps = 0.5$  is observed for  $x = 0.015$ , one can conclude that this composition is characterized by optimum combination of ferroelectric properties.

## 5. Conclusions

The structural, dielectric, and ferroelectric properties of bulk ceramic  $x\text{BiScO}_3-(1-x)\text{BaTiO}_3$  solid solutions with  $0.00 \leq x \leq 0.03$  were investigated. The samples were prepared by solid state reactions method at maximum heat treatment temperature of  $850^\circ\text{C}$ . Even at this low temperature it is possible to obtain stoichiometric solid solutions with tetragonal symmetry. Homogeneous distribution of principal elements, including Bi, over the sample surface was observed. Though the values of dielectric constant linearly increased with the doping level, optimum combination ferroelectric properties was found for  $x = 0.015$ .

## ACKNOWLEDGEMENTS

This work was supported by the Russian Foundation for basic Research (grant No. 08-02-99062\_r\_ofi), Program of the fundamental research of the Presidium of RAS No.21, Project of joint research of Ural and Siberian Branches of RAS No.09-S-2-1016, Program of the Department of physical sciences of RAS "Spin phenomena in solid-state structures and spintronics".

## REFERENCES

- [1] G.A. Smolensky, V.A. Bokov, V.A. Isupov, N.N. Kraynik, R.E. Pasynkov, A.I. Sokolov, N.K. Yushin. *Physics of Ferroelectric Phenomena*. Nauka, Leningrad. 1985 (in Russian)
- [2] Zou T., Wang X., Wang H., Zhong C., Li L., Chen I-W., 2008, Bulk dense fine-grained  $(1-x)\text{BiScO}_3-x\text{PbTiO}_3$  ceramics with high piezoelectric coefficient, *Appl. Phys. Lett.*, 93, 192913
- [3] Aleksandrov S. E., Gavrilov G. A., Kapralov A. A., Smirnova E. P., Sotnikova G. Yu., Sotnikov A. V., 2004, Relaxer Ferroelectrics as Promising Materials for IR Detectors, *Tech. Phys.*, 49(9), 1176-1180
- [4] Lemanov V. V., Smirnova E. P., Zaitseva N. V., 2009, Relaxors with Multiple Substitutions in Octahedral Sites of the Perovskite Structure V. V. Lemanov, *Phys. of the solid state*, 51(8), 1685-1690
- [5] Gorev M. V., Bondarev V. S., Flerov I. N., Sciau Ph., Savariault J.-M., 2005, Heat Capacity Study of Double Perovskite-Like Compounds  $\text{BaTi}_{1-x}\text{Zr}_x\text{O}_3$ , *Phys. of the solid state*, 47(12), 2304-2308
- [6] Jing Z., Yu Z., 2003, Crystalline structure and dielectric properties of  $\text{Ba}(\text{Ti}_{1-x}\text{Ce}_x)\text{O}_3$ , *J. Mater. Sci.* 38, 1057-1061
- [7] Ravez J., Simon A., 2000, Non-stoichiometric perovskites derived from  $\text{BaTiO}_3$  with a Ferroelectric Relaxor Behaviour, *Phys. Status Solid. A.*, 178, 793
- [8] Simon A., Ravez J., Maglione M. 2004, The crossover from a ferroelectric to a relaxor state in lead-free solid solutions, *J. Phys.: Cond. Matter.*, 16, 963-970
- [9] Simon A., Ravez J., Maglione M., 2005, Relaxor properties of  $\text{Ba}_{0.9}\text{Bi}_{0.067}(\text{Ti}_{1-x}\text{Zr}_x)\text{O}_3$  ceramics, *Solid State Sci.*, 7, 925-930
- [10] Ogihara H., Randall A., Trolier- McKinstry S., 2009, Weakly Coupled Relaxor Behavior of  $\text{BaTiO}_3\text{-BiScO}_3$  Ceramics *J. Am. Ceram. Soc.*, 92 (1), 110-118
- [11] Datta K., Thomas P.A., 2010, Structural investigation of novel perovskite-based lead-free ceramics:  $x\text{BiScO}_3-(1-x)\text{BaTiO}_3$ , *J. Appl. Phys.*, 107, 043516
- [12] Trolier- McKinstry S., Biegalski M.D., Wang J., Belik A.A., Takayama-Muromachi E., Levin I., 2008, Growth, crystal structure, and properties of epitaxial  $\text{BiScO}_3$  thin films, *Appl. Phys.*, 104, 044102-1-044101-7
- [13] Yao Zh., Liu H., Liu Y., Chen L., Hao H., 2009, Structure and ferroelectric properties in  $(\text{K}_{0.5}\text{Bi}_{0.5})\text{TiO}_3\text{-BiScO}_3\text{-PbTiO}_3$  piezoelectric ceramic system, *Matter. Res. Bulletin*, 44(7), 1511-1514
- [14] Hungria M., Amorin H., Alguero M., Castro A., 2011, Nanostructured ceramics of  $\text{BiScO}_3\text{-PbTiO}_3$  with tailored grain size by spark plasma sintering, *Scripta Mater.*, 64(1), 97-100
- [15] Li X., Zhu J., Wang M., Luo Y., Shi W., Li L., Zhu J., Xiao D., 2010,  $\text{BiScO}_3$ -modified  $(\text{K}_{0.475}\text{Na}_{0.475}\text{Li}_{0.05})(\text{Nb}_{0.95}\text{Sb}_{0.05})\text{O}_3$  lead-free piezoelectric ceramics, *J. Alloys and Compounds*, 499(1), L1-L4
- [16] Chuprunov E.V., Khokhlov A.V., Faddeev M.A.. *The Basics of Crystallography*. Editorial board for physical and mathematical sciences. Moscow. 2004. 500p. (in Russian)
- [17] Weast R. C., *Handbook of chemistry and physics, A Ready-Reference Book of Chemical and Physical Data*. CRC Press, Boca Raton, FL, 1976
- [18] Sun R., Wang X., Shi J., L. Wang. *Appl.*, 2011, Dielectric and polar order behaviors of  $\text{BaTiO}_3\text{-Bi}(\text{Mg}_{1/2}\text{Ti}_{1/2})\text{O}_3$  ceramics, *Appl Phys A*, 104, 129-133
- [19] Feng G., Rongzi H., Jia-ji L., Yong-hong Y., Chang-sheng T., 2008, Effect of different templates on microstructure of textured  $\text{Na}_{0.5}\text{Bi}_{0.5}\text{TiO}_3\text{-BaTiO}_3$  ceramics with RTGG method, *J.Europ. Cer. Soc.*, 28, 2063-2070
- [20] Cernea M., Andronescu E., Radua R., Fochib F., Galassib C., 2010, Sol-gel synthesis and characterization of  $\text{BaTiO}_3$ -doped  $(\text{Bi}_{0.5}\text{Na}_{0.5})\text{TiO}_3$  piezoelectric ceramics, *J. of Alloys and Compounds*, 490, 690-694
- [21] Bahri F., Simon A., Khemakhem H., Ravez, 2001, Classical or Relaxor Ferroelectric Behaviour of Ceramics with Composition  $\text{Ba}_{1-x}\text{Bi}_{2/3x}\text{TiO}_3$ , *Phys.Status Solidi A*, 184 (2), 459-464
- [22] Yasuda N., Kato T., Hirai T., Mizuno M., Kurachi K., Taga I.,

1994, Dielectric properties of  $\text{BaTiO}_3$ , Sr- and Pb-substituted  $\text{BaTiO}_3$  ceramics synthesized through hydrothermal method, *Ferroelectrics*. 154, 331

[23] Damjanovic D., 1998, Ferroelectric, dielectric and piezoelectric properties of ferroelectric thin films and ceramics, *Rep. Prog. Phys.*, 61, 1267–1324